

### NEOTECTONICS

Neotectonics is the study of crustal movements that occurred in the recent past and continue till today. These movements, which are driven directly or indirectly by global plate motions (tectonics), result in the vertical and horizontal warping, folding or faulting of the Earth's surface. To get a complete picture of the pattern of neotectonic movements across both time and space for a particular region a multidisciplinary approach is must. The seismic hazard studies are based on the knowledge of the neotectonics of an area. Due to the societal importance of the results of neotectonic studies, considerable attention is given in acquiring, processing, and interpreting the data.

Neotectonic studies in the lower Narmada basin particularly along Narmada-Son Fault (NSF) have been singularly lacking. The present study was therefore aimed at understanding the nature of neotectonic activity along the NSF and its role in shaping the present landscape of the lower Narmada basin. The lower Narmada basin astrides the Narmada-Son Fault (NSF), an important ENE-WSW trending tectonic element responsible for the current intraplate seismicity being experienced in the central part of the Indian plate. The subsurface data gives only a rough estimate of the tectonic evolution as it is principally based on the thickness of Quaternary sediments (Figs. 2.5, 2.6B, 2.7). The evidence indicating Late Quaternary neotectonic activity in lower Narmada basin are geomorphic and stratigraphic evidence including sediment deformation in alluvial plain sediments.

#### GEOMORPHIC EVIDENCE

The geomorphic evidence observed in the lower Narmada basin are the young mountain front scarps delimiting the basaltic uplands and marking the Narmada – Son Fault, youthful

channel morphology of the Narmada and other rivers as testified by consistent presence of incised vertical cliffs, entrenched meanders, extensive and deep ravines, uplifted Holocene terraces, anomalous slope variations specially to the south of Narmada, remarkable correlatability of the drainage with structural features in low Tertiary uplands (Figs. 2.6, 3.3). The earthquakes along the length of the NSF indicate that the neotectonic movements still continue. Varying nature and degree of tectonic movements along the NSF during Late Pleistocene and Holocene have produced four geomorphic surfaces (described in earlier sections) in the lower Narmada valley – the alluvial plain ( $S_1$ ), ravine surface ( $S_2$ ), a gravelly fan surface ( $S_3$ ) and the valley fill terrace surface ( $S_4$ ). Differential uplift along NSF resulted in the erosion of the Late Pleistocene sequence and formation of a deeply incised fluvial valley during Early Holocene, a period of sea level rise. Evidence of this tectonic uplift is observed in the displacement of the alluvial plain surface across NSF, NNW tilting of the sediments in the vicinity of NSF (Fig. 3.5) and the incised cliffs of about 30-40 m along the lower Narmada valley (Fig. 3.21). The fault bound Rajpipla block subsided at this time resulting in deposition of alluvial fans over the Late Pleistocene sediments which coalesced to form the  $S_3$  surface (Fig. 4.16A). The Mid-Late Holocene high sea led to the deposition of estuarine sediments in the lower reaches (Fig. 3.22) and fluvial sediments in the upstream reaches as valley fill terraces (Fig. 3.23). Incision of 5-12 m and tilting of these terraces near NSF indicate differential uplift along NSF during Late Holocene.

#### **Qualitative Geomorphic Analyses**

Detailed morphometric studies were carried on Karjan river basin a tributary of Narmada River (Raj et al. 2003) in the lower reaches to substantiate the field data on active tectonics using topographic maps at 1:50,000 scale. Morphometric parameters such as sinuosity, long profiles, valley floor to valley width ratios and mountain front sinuosity characterise the degree and nature of tectonic activity whilst stream orientation studies help in reconstructing the sequence of recent tectonic activity (Centamore et al. 1996). The orientations related to lower order streams are indicative of the most recently active tectonic phase because these streams are the youngest component of the drainage network (Centamore et al. 1996).

The Karjan river basin, a tributary basin of the lower Narmada valley which provides ample evidences of active tectonism in the landscape evolution was chosen for qualitative assessment of the neotectonism in the lower Narmada basin (Raj et al. 2003). Three tilt blocks within a larger tilt block are delineated in the upland zone which have been formed due to differential uplift along the Narmada-Son Fault and two other faults with similar trends (Raj et al. 2003) (Fig. 3.5). There is a close correspondence between these faults and major landform discontinuities. The prominent north facing escarpments, ENE-WSW trending narrow intramontane valleys, general decrease in the ruggedness of the topography towards south, preferential locations of river ponding, gorges and fluvial incision indicate continued southward

tilting of the fault blocks in Recent times due to differential uplift. Valdiya (2001) has also indicated river ponding in the rivers of Sahyadri as the key evidence for neotectonic activity and related it to differential movement along the faults.

### **Lineament Analysis**

Lineament analysis of the Karjan River basin was carried out by the visual interpretation of IRS FCC images in conjunction with the Survey of India toposheets and field checks. The lineaments have been picked up on the basis of trends of morphological features, structural alignments, textural contrasts and tonal differences. The drainage courses have also been considered as lineaments because of their preferred orientations and meander patterns. The lineament pattern of the Karjan basin indicates strong control of ENE-WSW and NNW-SSE tectonic trends on the drainage architecture (Fig. 6.1). However, the ENE-WSW trend appears to have significantly influenced the fluvial geomorphology and the overall topography of the basin.

Apart from the dominant ENE-WSW geomorphic grain of the area, the lineaments

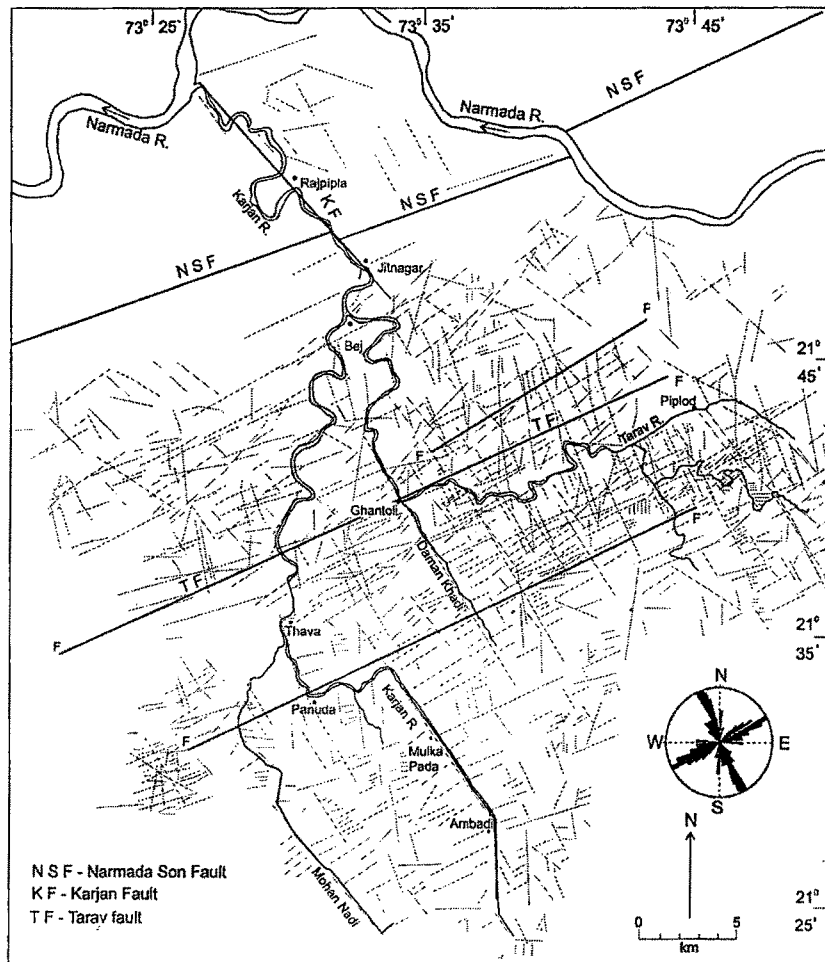


**Fig. 6.1.** Major faults and lineaments in the Karjan basin with rosette showing the dominant lineament trends

indicate a prominent NNW-SSE tectonic trend. These two tectonic trends are uniformly observed all over the Deccan Volcanic Province (Powar, 1980; Widdowson and Mitchell, 1999) suggesting that the stress patterns which affected the Peninsular India has affected the Karjan basin also. The course of the Karjan River and its tributaries the Tarav, Mohan Nadi and Daman Khadi show a distinct structural control (Fig. 6.1) of these two tectonic trends. Many of the higher order streams like the Karjan, Tarav and Dhaman Khadi (Fig. 6.1) show a strong control of NNW-SSE trending lineaments, however, no geomorphic evidence of faulting was found along these lineaments during this study. The dominance of the ENE-WSW trend in the geomorphic set up can be attributed to the presence of the neotectonically active Narmada-Son Fault within the Karjan basin (Fig. 6.1). Another reason for the influence of this trend on geomorphology is the presence of two other faults parallel to the Narmada-Son Fault (Fig. 6.1). These faults divide the major tilt block into three smaller tilt blocks with prominent geomorphic expressions of the type described above. One of these faults is the westward extension of the Tarav fault, which controls the upper course of the Tarav River. Presence of several springs and waterfalls along this line is further indicative of the presence of a fault. The Tarav River takes an abrupt turn at Ghantoli to meet the Karjan River at Bej (Fig. 3.7). This change in the course of the Tarav River is attributed to a NNW-SSE trending lineament (Fig. 6.1) which also controls Daman Khadi, a tributary of Tarav River. The second fault is located further south which is also marked by a north facing escarpment. The remarkably straight NNW-SSE course of the Karjan shows an abrupt westward deflection, which has been caused by tilting due to differential uplift along this fault. The fresh nature of escarpments marking these faults indicate that differential uplift along the faults have kept pace with the erosional processes so that the topography still mimics the original nature of the tilt blocks. These are seen extending for several kilometers occurring as straight wall like fronts (Fig. 3.5).

### ***Stream Orientation***

The Karjan River basin can be described as a narrow and asymmetrical basin (Fig. 6.2). The Karjan River is a 7<sup>th</sup> order stream and covers a total basin area of 1523 km<sup>2</sup> with altitudes ranging from 30 to 600 m amsl. The streams of the Karjan basin show a rectilinear pattern that has resulted from preferential drainage along a pre-existing NNW-SSE and ENE-WSW lineaments (Fig. 6.1). The streams flowing through the basaltic upland follow joints and faults carving a conspicuous criss-cross meander course (Fig. 6.2). At places the streams of the Karjan and Tarav Rivers are conspicuous by their 5-8 km long NNW-SSE trending straight courses controlled by the lineaments (Fig. 6.1). The overall drainage orientations show a subdued influence of ENE-WSW trending lineaments. The stream orientations show that the 1<sup>st</sup>, 2<sup>nd</sup> and 3<sup>rd</sup> order streams trend dominantly in NNW-SSE and quite a few in ENE-WSW directions. The

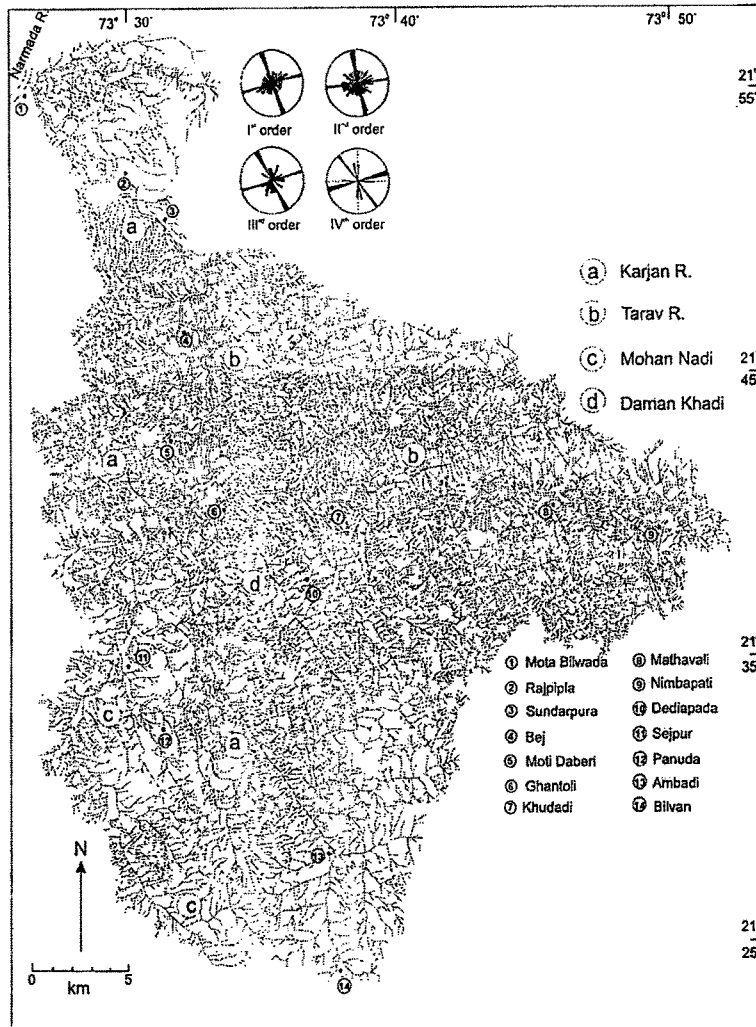


**Fig. 6.2.** Drainage map of Karjan basin with tributary sub-basins. Note the control of NNW-SSE trending lineaments on drainage

stream orientation analysis has revealed that the lower order streams are dominantly controlled by NNW-SSE trending lineaments (Raj et al. 2003).

#### *Long Profile Analysis*

River response to active tectonism is reflected in longitudinal profile of the river (Rhea, 1993), and the comparison between longitudinal profiles are made using Pseudo Hypsometric Integral (PHI). PHI reflects the relative amount of

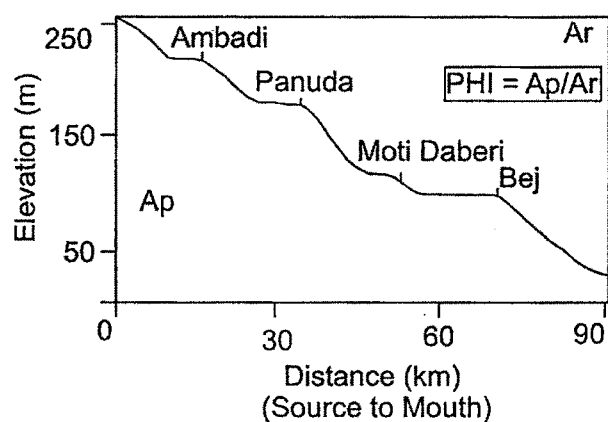


**Fig. 6.3.** Longitudinal Profile of Karjan River showing prominent breaks at Ambadi, Panuda, Moti Daberi and Bej

deformation or degradation that has occurred on each river (Rhea, 1993). The pseudo-hypsometric integral (PHI) is calculated by numerical means ( $PHI = A_p/A_r$  expressed in percentage), where  $A_p$  is the area under the long profile and  $A_r$  is the area of the rectangle defined by total height and length of the river basin which describes the overall shape of the long profile. High value of pseudo hypsometric integral (50) indicate that the basin have been rejuvenated in recent times (Raj et al. 2003). Further, the long profiles of the Karjan and Tarav rivers

show prominent breaks at Ambadi, Panuda, Moti Daberi and Bej (Fig. 6.3) and at Nimbapati, Mathavali, Khudadi, Ghantoli and Bej (Fig. 6.4), respectively.

#### **Gradient Index and Valley Floor Ratio**

Gradient Index is an important morphometric parameter which helps in identifying areas that have undergone differential uplift. It is calculated by measuring the elevation change over a logarithmically normalised distance using the formula (Rhea, 1993) -

$$\text{Gradient Index (G. I.)} = \frac{h_1 - h_2}{\ln l_2 - l_1}$$

where,  $h$  is elevation and  $l$  is the distance.

The values thus obtained are plotted against distance from source to mouth. The values of gradient index for the Karjan basin are found anomalously high wherever it passes through the faults (Raj et al. 2003) (Fig. 6.5). The higher values of gradient index in the alluvial zone near its

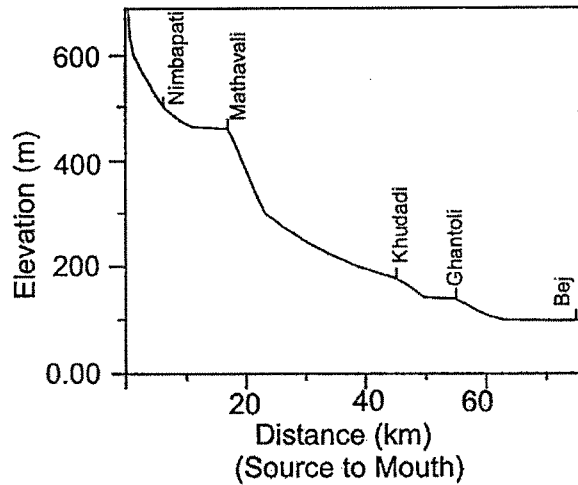


**Fig. 6.4.** Longitudinal Profile of Tarav River showing prominent breaks at Nimbapati, Mathavali, Khudadi, Ghantoli and Bej

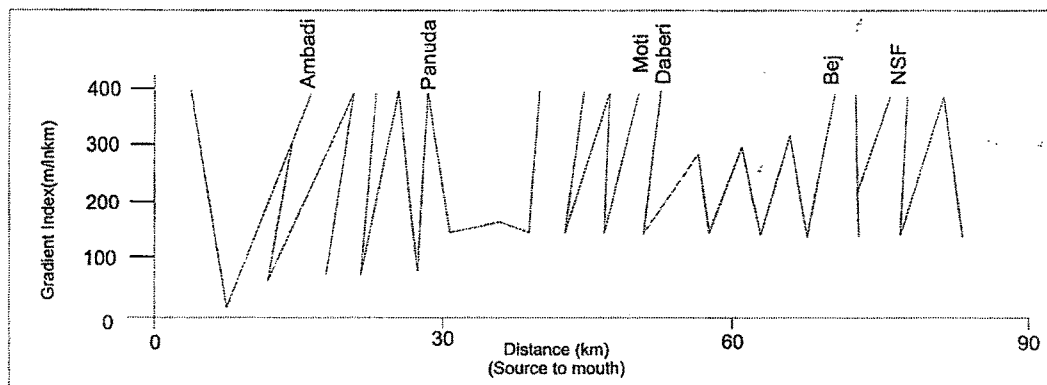


**Fig. 6.5.** Plot of Gradient Index of Karjan River

confluence with Narmada are due to the Late Holocene uplift along the Narmada-Son Fault (Bhandari et al. 2001).

The valley floor width (Vfw) and valley height (Vht) ratios were determined with a view to identify the areas of tectonic quiescence and areas that have been uplifted recently. The valley floor (Vf) ratios (calculated by dividing valley floor width by valley height) of the Karjan basin were calculated at every 3 km interval (Fig. 6.6). The high valley-floor width to valley-height and low valley-floor width to valley-height ratios have been attributed to tectonic quiescence and recent tectonic movements, respectively (Mayer, 1986). Valley incision has also been used to define relative uplift (Bull and McFadden 1977; Ouchi, 1985; Rhea 1993).

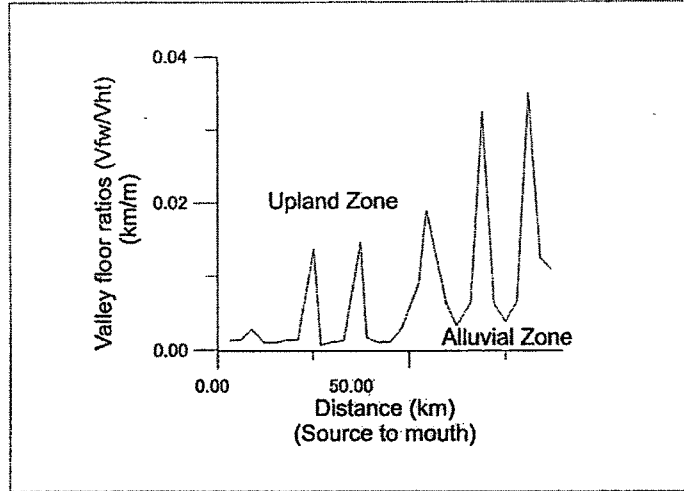


Fig. 6.6. Valley floor ratios of Karjan River

#### ***River Sinuosity***

Any deviation of the river course from a straight line is termed as sinuosity. The sinuosity of a river is the result of factors like tectonism and hydraulic factors. Higher sinuosities of rivers are attributed to higher tectonic activity. In response to uplift a river changes its channel pattern by increasing sinuosity or by changing channel pattern to straight or braided (Burnett and Schumm, 1983; Ouchi, 1985). Muller (1968) proposed to evaluate the relative roles of topographic and hydraulic factors in shaping the channel morphology of rivers. He introduced two new parameters the Topographic Sinuosity Index (TSI) and the Hydraulic Sinuosity Index (HSI), which are expressed as percentage. A higher value of TSI over HSI is generally taken as indicative of rejuvenation i.e. the tectonic factor dominating over hydraulic factor. This is based on the premise that the topography in drainage basins is provided by rejuvenation i.e. tectonic uplift. These indices are useful in deducing the controlling factor of river sinuosity.

The various indices of sinuosity are determined using the following formulae:

$$\text{SSI (Standard Sinuosity Index)} = \frac{\text{CL}}{\text{VL}}$$

Where CL is average of the lengths of the channel measured along both banks, VL is length of valley between the base of the valley walls.

$$\text{HSI (Hydraulic Sinuosity Index)} = \frac{\text{CI}-\text{VI}}{\text{CI}-1} \times 100$$

Where CI is channel index determined by dividing the channel length by air length (CI= CL/AL) and VI is valley index determined by dividing valley length by air length (VI=VL/AL).

$$\text{TSI (Topographic Sinuosity Index)} = \frac{\text{VI}-1}{\text{CI}-1} \times 100$$

Karjan River basin has shown high values of TSI as compared to HSI (Fig. 6.7) and these high values correspond well with the faults in the area indicating dominance of tectonic factor over hydraulic factor (Raj et al. 2003).

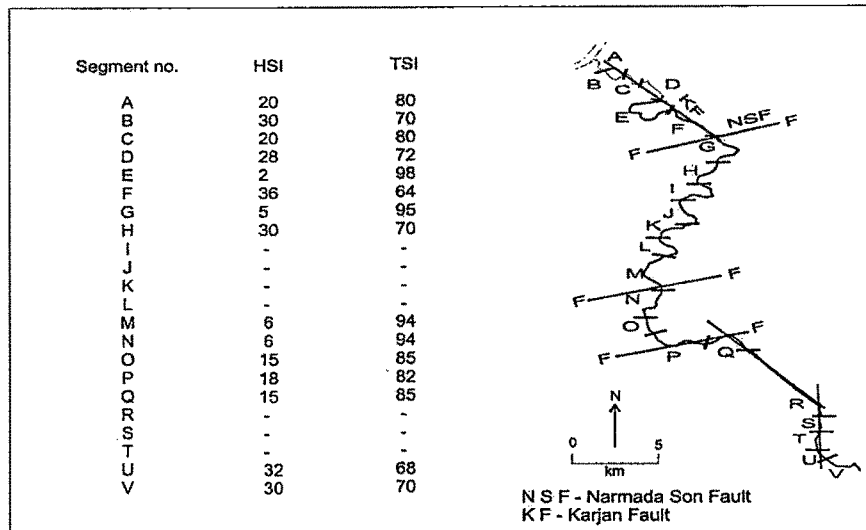


**Fig.6.7.** Sinuosity values of Karjan River computed for segment indicated

### ***Mountain Front Sinuosity***

Mountain Front Sinuosity is an index of the degree of irregularity of sinuosity along the base of a topographic escarpment (Wells et al. 1988). Active fronts maintain straight or curvilinear profiles in plan view as contrasted to the more irregular profiles produced by erosional processes along the base of associated topographic escarpments. The degree of tectonic activity and the erosional modification of tectonic structure can be measured by mountain front sinuosity index using the following formula.

$$\text{Mountain front sinuosity (S)} = \frac{\text{Lmf}}{\text{Ls}}$$



Where  $L_{mf}$  is the length of the topographic mountain front and  $L_s$  is the shortest length that parallels or circumscribe overall mountain front. Mountain front sinuosity ( $S$ ) was determined for the selected areas following Bull (1978, 1984) in the Karjan basin (Fig. 6.8). The sinuosity values of steep scarp like mountain fronts of the Narmada-Son Fault zone fall in the tectonic activity class 1 of

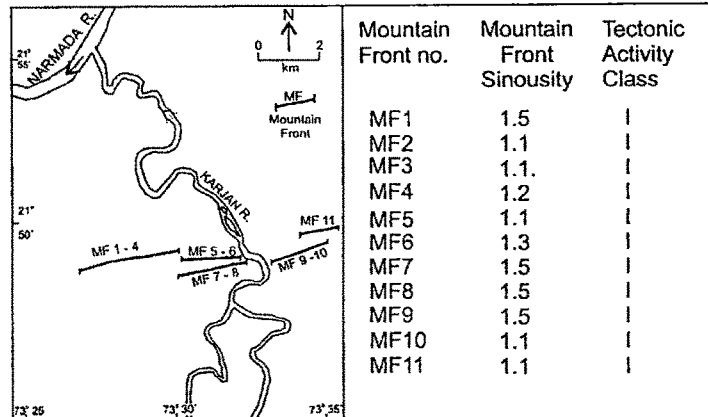


**Fig.6.8.** Map showing location of mountain fronts analysed and the values of Mountain Front Sinuosity (the tectonic activity class is after Bull & McFadden, 1977)

Bull and McFadden (1977) pointing towards active tectonism in the area (Raj et al. 2003).

#### ***Ravine Orientations***

The ravine areas form an important part of the geomorphology of the Lower Narmada basin. Ravine erosion has been attributed to various causes like climatic changes, catastrophes, isostatic rebound and tectonic uplift (Bull, 1964, Ahmed, 1968, Ouchi, 1985, Pant and Chamyal, 1990). The ravine areas in lower Narmada are made up of unconsolidated and consolidated alluvial sediments. Flat alluvial plain on one side and the river channel on the other delimit the ravine area. The sediments that make the ravine surface dates back to Late Pleistocene. The younger terraces were deposited during Middle to Late Holocene which do not show any sign of ravine erosion. The ravine erosion thus took place after the deposition of Late Pleistocene sediments and before the deposition of Middle Holocene terraces (Maurya et al. 2000). The ravines are the result of a tectonic uplift aided severe erosional phase. The analysis of ravine orientations was carried out to investigate the role of ENE-WSW trending Narmada-Son Fault (NSF) in the evolution of these ravines (Fig. 6.1).

This analysis was carried out using the Survey of India topographical maps on 1:50,000 scale. To facilitate the ravine analysis, the area was divided into grids of equal sizes. The orientations of the first and second order ravines were measured separately and rosettes were prepared for each grid (Fig. 6.9). Each finger tip ravine was considered as the first order. The trunk ravine in which the various first order ravines join are considered to be of second order (Raj et al. 1999). As seen in the rosettes (Fig. 6.9), the first order ravines show-varying trends. However, the second order ravines, which are in fact, the trunk ravines show a preferred E-W trend, which matches with the regional tectonic trend. The dominant trend of the ravines also shows striking similarity with the major lineament trend of the area. This suggests that the

formation of ravines is tectonically controlled and that the tectonic activity along the Narmada trend is responsible for the extensive ravine erosion in the Lower Narmada basin. Raj et al. (1999) have also related the ravine formation to neotectonism in the Mahi basin.

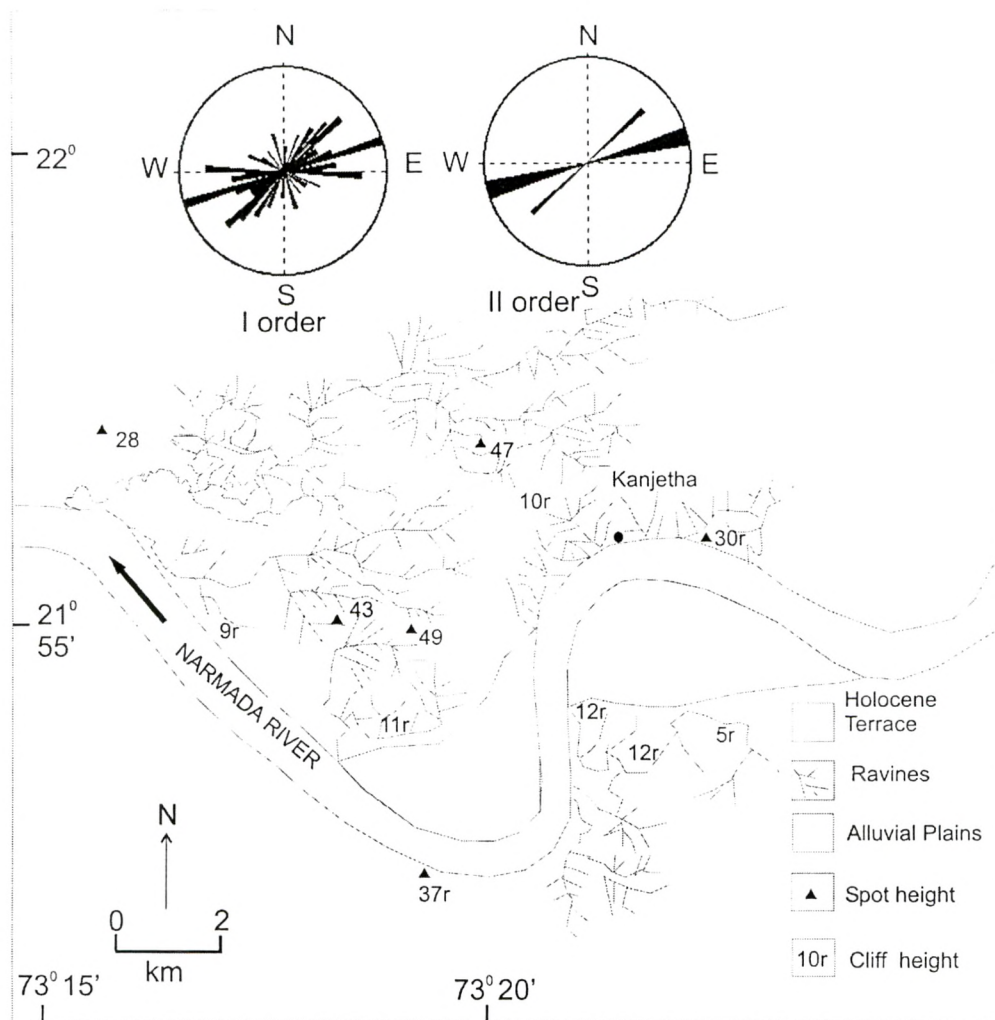


**Fig. 6.9.** Ravines of the lower Narmada basin with rosettes showing dominant ravine trends

The field studies are well supported by the morphometric parameters. The lower order streams show a dominant influence of NNW-SSE trending lineaments. Significantly, the main course of the Karjan River also follows this trend. ENE-WSW faults and lineament trends, perhaps conditioned the major geomorphic set up of the Karjan basin and drainage network during Early Holocene. The longitudinal profile of the Karjan River shows variable slopes. The lower order streams show steep cliffy slopes and entrenchment in their channels, which are indicative of uplifts. A relatively high value of PHI (50) and variable values of valley floor width to valley height ratios further point to recent tectonism in the basin (Mayer, 1985). Along with downcutting and deposition, a river may respond to uplift by changing channel patterns, such as

by increasing sinuosity (Burnett and Schumm, 1983; Ouchi, 1985). Values of Topographic Sinuosity Indices (TSI) mainly in the segments following faults are high. These values not only confirm the occurrence of fault controlled courses but also point to their active nature (Muller, 1968; Rhea, 1993). The differential uplift is further supported by the gradient index values of the main Karjan River which are highly variable from source to mouth. Mountain front sinuosity values further support that the area has been experiencing active tectonism. The field data is well substantiated by morphometric parameters and point to differential uplifts along ENE-WSW faults in the Karjan river basin during Holocene (Raj et al. 2003).

The Late Quaternary tectonic events have also played a significant role in the geomorphic evolution of the Karjan basin. These events are recorded in the alluvial basin to the north of the Narmada-Son Fault (Maurya et al. 2000; Bhandari et al. 2001; Chamyal et al. 2002). Neotectonic activity during Early Holocene along the ENE-WSW trending Narmada-Son Fault which provides geomorphic contrast in the Karjan basin resulted in the deposition of a number of alluvial fans which have coalesced and formed a distinct geomorphic surface (Bhandari et al. 2001). During Mid to Late Holocene, there was yet another event of tectonic uplift (Maurya et al. 2000; Bhandari et al. 2001) leading to the upliftment of the terraces. Fluvial terraces in the upland zone and alluvial zone of the Karjan basin occur at varying heights (5-8 m), indicating tectonic uplift in the basin during Late Holocene. Generally, formation and preservation of river terraces without significant uplift is considered to be unlikely (Veldkamp and Vermeulen, 1989; Veldkamp and Vandenberg, 1993), the incision in the young terrace surfaces of the basin is, therefore, linked with latest tectonic uplift in the basin. Similar evidence of Recent uplift in the Maharashtra Deccan uplands are noted by Widdowson and Mitchell (1999).

## **STRATIGRAPHIC EVIDENCE**

### **The alluvial fan sediments**

The presence of alluvial fan facies in the sediment record is generally taken as direct evidence of a tectonic activity (Steel et al. 1977; Heward, 1978). Optimal conditions for fan development are created in regions undergoing extension (Blair and Bilodeau, 1988) such as the western North American Basin and Range province, the Middle Eastern Dead sea rift and the East African rift system. Extensional basin settings are especially conducive for long term fan development leading to deposition of fan sequences hundreds of meters thick where as long term development of fans is hindered in compressive tectonic regimes owing to greater strong component of lateral tectonic deformation (Blair and McPherson, 1994). The transformation of the Narmada-Son Fault from a normal fault in Tertiary to reverse fault in Quaternary is implicit in the seismic studies of the area (Roy, 1990). Additional evidence for prevalence of compressive stress regime in the Lower Narmada basin is provided by numerous reverse faults (Fig. 2.6) in the Neogene sediments exposed immediately to the south of Narmada-Son Fault (Agarwal, 1986).

These evidences suggest that both the fans, Fan 1 and 2 were formed in a compressive tectonic environment. This could be the reason for the fact that the maximum thickness of the fan sequences is about 70-80 m only of which about 35 m is exposed. This compares well with the observation of Blair and McPherson (1994) that fan development is hindered in compressive tectonic settings. The existence of compressive stress regime affected the fan morphology due to which both fans show a rather elongated fan shape resulting in alluvial fans of unusual axial lengths (Chamyal et al. 1997). The alluvial fan sediments are overlain by a thick sequence of alluvial plain facies which indicate termination of fan sedimentation and initiation of riverine sedimentation by a more integrated drainage system.

### **The alluvial plain sediments**

The alluvial plain sediments mark an abrupt change in type and style of sedimentation. These sediments are mainly fluvial sands and silts which is in contrast with the underlying coarse sediments of the alluvial fan facies. Evidences of tectonic influences during the deposition of these sediments are seen in the form of tectonically induced deformation structures and the overall sediment characteristics. Several studies exist which document effects of synsedimentary subsidence on the alluvial plain sedimentation (Schuster and Steidtmann, 1987; Brown and Plint, 1994; Kraus and Middleton, 1987; Kraus, 1992; Jordan, 1981; Hagen et al. 1985). Absence of soil profiles in the thick overbank fines of the study area is indicative of synsedimentary subsidence of the basin. Soils can only develop on land surfaces which are relatively stable (Ruhe, 1956; Bull, 1991; Marriot and Wright, 1993). The facies associations contain no pervasive fining upward trends or lateral accretion features suggesting no major deviations in the mean flow directions.

It is unlikely that a high sinuosity channel will produce stacked system of fluvial deposits showing these characteristics (Schuster and Steidtmann, 1987). Deformation in these sediments of the types described below are the direct manifestations of this subsidence. Strong similarity of the structural orientations of the deformation structures suggest subsidence in a thrusting environment along the NSF which is consistent with the subsurface studies. A study by Schuster and Steidtmann (1987) in a structural setting similar to the present area of study, demonstrated that sand bodies with high degree of persistence and interconnectivity are expected during low subsidence rates while the converse is true in case of rapid subsidence. Therefore it can be inferred that a low sinuous and relatively fixed river system in a slowly subsiding basin lead to the deposition of these sediments. Geomorphic stability was attained after the phase of overbank sedimentation as indicated by the pedogenic alteration of the top of the overbank sequence resulting in the formation of a thick red soil.

### ***Sediment Deformation***

A wide variety of deformation structures are observed in the exposed sediments of the lower Narmada basin (Chamyal et al. 2002). The deformation structures observed in the Late Pleistocene sediments are - intraformational folds and flexures, slump structures, joints some showing small scale offsets and large vertical fractures affecting entire cliff sections and tilting.

#### **Intraformational folds**

The most commonly observed deformational features are the intraformational folds in the well stratified over bank sediments overlying the alluvial fan deposits. The folds are observed at scales ranging from centimeters to several tens of meters. These occur in the form of small



**Fig. 6.10.** Intraformational open folds in the overbank deposits at Ambali (height of the person is 1.65m)

symmetrical folds to wide-open flexures (Fig. 6.10) with wide-open anticlines and synclines. The dips of the fold limbs vary from  $50^{\circ}$  to as low as  $8-10^{\circ}$ . Since the folds are seen in overbank deposits which are normally laid down in almost perfectly horizontal manner, a tectonic factor is implied for the folding (Chamyal et al. 2002).

Moreover, the fold axis in all sections studied trend in  $N 50^{\circ}$  to  $N 80^{\circ}$  which is consistent with the regional tectonic trend. The overlying and underlying sediments do not show the effects of folding suggesting penecontemporaneous tectonic deformation during the rapid phase of overbank sedimentation.

#### **Synsedimentary faults**

Small scale (centimeter scale) synsedimentary faulting is observed in these sediments. All fault planes are found to be consistently oriented in ENE-WSW direction. Majority of the fault planes exhibit low southward dips ( $10-25^{\circ}$ ) and show reverse movement and hence can be categorised as low angle thrust faults (Fig. 6.11). The displacement of the strata is in the range of





**Fig. 6.11.** Small-scale low angle thrust fault in the overbank deposits at Nava Tavra (length of the pencil is 12 cm.) 5-10 cm. These faults suggest a northward directed compressive stresses from the south (Chamyal et al. 2002).

### Fractures and joints

Fractures and joints run for few meters to few tens of meters. Vertical fractures affecting the entire cliffs are also observed (Fig. 6.12). These fractures are found to be filled with secondary clay and silt. The fractures also show dominant ENE-WSW trend while a few trend in NNW-SSE direction. Some fractures exhibit displacement on millimeter scale. The fracture pattern also conforms to the regional tectonic trend.

### Slumps

Synsedimentary slumps are found to occur in the alluvial plain sediments. The slumps vary in dimension from 1 to 10 m. These slumps show a well-defined slump plane which shows a consistent trend of ENE-WSW (Fig. 6.13). The overlying sediments show no effect of slumping indicating the synsedimentary nature of the slumps. The consistent



**Fig. 6.12.** Horizontal as well as vertical jointing seen in the Late Pleistocene sediments with deposition of calcretes along joints. See the minor deflection in the joints

trend of the slumps conforming to the regional trend strongly suggests that they are part of the syndepositional tectonic deformation (Chamyal et al. 2002).



**Fig. 6.13.** Syndepositional slump structure in the alluvial plain sediments at Patan (height of the person is 1.65m)

### Tilting

Tilting is observed in Late Pleistocene as well as the Mid-Late Holocene terrace sediments. The Late Pleistocene sediments show NNW tilt (Fig. 6.14) of 5-15° which is more pronounced in the incised cliff sections of the streams joining the Narmada from the south. This is well evidenced by stratigraphically correlatable Late Pleistocene sediments attaining heights of 80-100 m in the vicinity of the NSF while along the Narmada River, these sediments occur at an elevation of 40-60 m. Since the entire sediment column is tilted, this is very well reflected in the topographic slope of

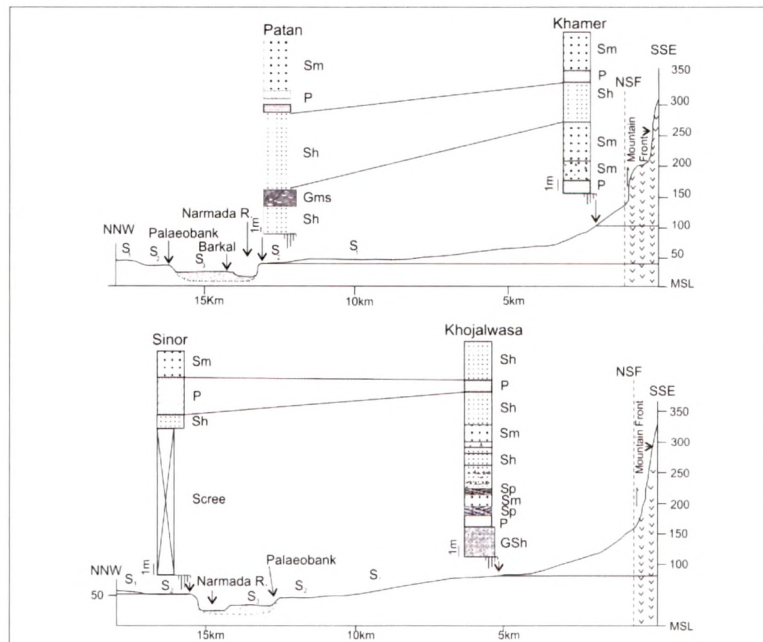


**Fig. 6.14.** Topographic profiles showing postdepositional tilting of the S<sub>1</sub> surface consisting of Late Pleistocene sediments

the area between the NSF and the Narmada River. This also suggests that the tilting is post-depositional i.e. post Late Pleistocene which can be attributed to differential uplift along the NSF (Chamyal et al. 2002).

#### **Offset along NSF**

The  $S_1$  surface shows anomalous NNW slope between the Narmada River and the NSF (Fig. 6.14). The difference in the elevations of the Late Pleistocene sediments comprising this surface on either sides of the NSF in the Narmada and Karjan valleys suggest an offset of about 35 m. The sediments of  $S_1$  surface occur at elevations upto 100 m across the NSF as seen near Gora (Fig. 3.17, 3.20) in Narmada valley and Jitnagar in Karjan valley in the Narmada and Karjan valleys respectively. At these places, these sediments occur well above the present high discharge levels and overlie the basalts, which also show vertical downcutting by the river. The  $S_1$  surface, generally attain elevations of 30-40 m along the Narmada River. NNW directed tilting of these sediments observed in the area to the south of Narmada provides additional evidence for differential uplift along the NSF. However, the Mid-Late Holocene sediments ( $S_4$  surface) do not show any observable offset along the NSF suggesting that the offsetting of the  $S_1$  surface took place during the Early Holocene phase of tectonic uplift. The displacement of the  $S_1$  surface point to a differential movement of about 35 m along the NSF during Early Holocene (Chamyal et al. 2002).

#### **Seismically Induced Soft Sedimentary Deformation Structures**

The tectonically aided great erosional phase was followed by the Middle to Late Holocene aggradation which commenced at ~6000 yr B.P. The Mid-Late transgression was within the incised fluvial valley which resulted in estuarine sedimentation in the lower reaches and fluvial in the upper reaches. Seismically induced soft sediment deformation features from comparable terrace sediments in Mahi valley (Maurya et al. 1998) and Orsang valley (Maurya et al. 2000) suggest tectonic instability of the region during the period of valley fill sedimentation (Fig. 6.15). Deformation structures have also been observed around Amrawati River (Fig. 6.16) a tributary of Narmada River meeting it from the south.

Existing data suggest that the Mid-Late Holocene sea level has remained at the same level upto the present with minor fluctuations (Hashimi et al. 1995). Radiocarbon dates from the adjoining Mahi basin also indicate that uninterrupted marine sedimentation took place upto  $1760 \pm 80$  yr B.P. in the estuarine zones (Kusumgar et al. 1998). The Holocene sediments show tilting of  $10-20^\circ$  which is more pronounced in the vicinity of the NSF suggesting that the incision and upliftment of the valley fill terraces well above the present day tidal limits is related to the continued differential uplift along NSF. Additional evidence in this respect is provided by present channel belt of the Narmada River which occupies the northern portion of the much wider channel it carved out during the Early Holocene.



Two major phases of tectonic movements in a compressive stress regime are recorded along the NSF – slow synsedimentary subsidence of the basin during Late Pleistocene due to differential movement



**Fig. 6.15.** Load structures formed due to seismic loading in a fluvial Holocene terrace in the Orsang valley at Anklawadi

followed by inversion of the basin during the Holocene marked by differential uplift along the NSF (Chamyal et al. 2002).

The study suggests that the inversion of the basin is in response to the significant increase in the intensity of compressive stresses in the Indian plate mainly during the Early Holocene. The present incisive drainage and recent seismic activity indicates that the compressive stresses continue to accumulate along the NSF due to continued northward movement of the Indian plate.

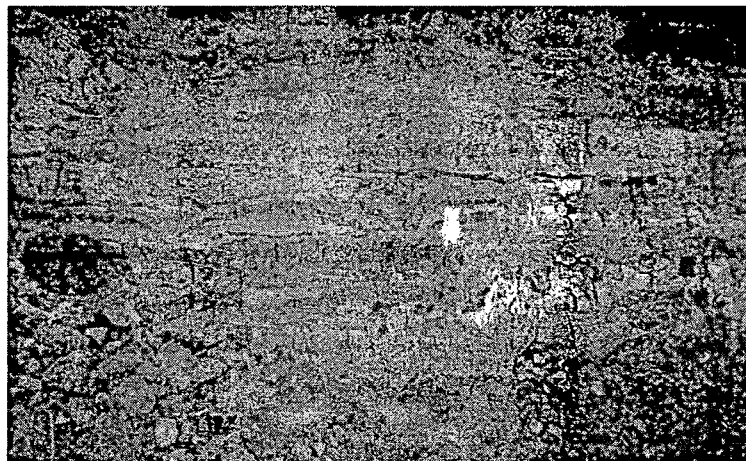


**Fig. 6.16.** Photograph showing soft sediment deformation structures seen in sand and clay in Amrawati River at Dhadal